11-1-2023

Air-side fouling of finned heat exchangers: Part 2, experimental demonstration and assessment of test protocol

Justin Weibel
jaweibel@purdue.edu

Weibel, Justin, "Air-side fouling of finned heat exchangers: Part 2, experimental demonstration and assessment of test protocol" (2023). *CTRC Research Publications.* Paper 413.
http://dx.doi.org/https://doi.org/10.1016/j.ijrefrig.2023.03.016

International Journal of Refrigeration 151 (2023) 63–76

Contents lists available at ScienceDirect

International Journal of Refrigeration

journal homepage: www.elsevier.com/locate/ijrefrig

Review

Air-side fouling of finned heat exchangers: Part 2, experimental investigation and assessment of test protocol

Encrassement côté air des échangeurs de chaleur à ailettes : Partie 2, Étude expérimentale et évaluation du protocole d'essai

Harshad V. Inamdar [a], Eckhard A. Groll [b,*], Justin A. Weibel [b], Suresh V. Garimella [b]

[a] Rheem Manufacturing Company, Fort Smith, AR 72908, USA
[b] Purdue University, School of Mechanical Engineering, Cooling Technologies Research Center, West Lafayette, IN 47907, USA

ARTICLE INFO

Keywords:
Particulate fouling
Heat exchanger
Air-side fouling
Finned microchannel
Test protocol
Mots clés:
Encrassement particulaire
Échangeur de chaleur
Encrassement côté air
Microcanal aileté
Protocole d'essai

ABSTRACT

An experimental test protocol for simulating the air-side fouling of heat exchangers, as well as metrics to characterize the extent of fouling undergone by the heat exchanger and its performance in clean and fouled conditions, were proposed in a companion paper. In this study, the air-side fouling of a finned microchannel heat exchanger is experimentally investigated according to the proposed protocol. Key test parameters influencing heat exchanger fouling are identified based on studies in the literature, and their impact is experimentally investigated. The effectiveness of *in situ* cleaning methods is also experimentally evaluated. Transient measurement data and photographs taken during the fouling process reveal the nature of fouling, while steady-state data quantify the degradation in heat exchanger performance due to fouling. This two-part study defines a generalized experimental approach to enable characterization and comparison of heat exchanger surfaces on a standardized basis, and provides detailed experimental data for modeling heat exchanger fouling that includes all necessary information to allow for model validation.

1. Introduction

A detailed literature review in the companion Part 1 of this two-part paper (Inamdar et al., 2023), identifies the lack of a standardized, repeatable test procedure to experimentally foul heat exchangers and evaluate their performance in a fouled condition. To fill this gap in the literature, an experimental test protocol, along with a method to quantify heat exchanger fouling and metrics to quantify heat exchanger performance before and after fouling, are proposed.

Deposition on surfaces from a moving fluid is hypothesized as occurring in three stages by Bott (Bott, 1995):

1 Transport of the foulant across the boundary layers adjacent to the deposition surface within the flowing fluid;
2 Adhesion of the deposit to the surface and to itself; and
3 Transport of material away from the surface.

Different mechanisms are proposed for each stage; multiple operating and geometric parameters are expected to affect each mechanism. Under isothermal conditions, inertia, diffusion (Brownian and eddy), and gravitational settling are responsible for transportation of the foulant from bulk flow to the deposition surface. Under non-isothermal conditions, thermophoresis and diffusiophoresis are additional relevant mechanisms. Intermolecular forces such as van der Waals forces and electromagnetic forces are proposed to affect agglomeration of foulant layers. Shear-induced re-entrainment of particles and local flow instabilities due to surface asperities may transport particulates away from the surface. Properties of the fluid and foulant, flow characteristics, surface geometry, and interactions between the fluid, foulant, and surface are all expected, in some measure, to dictate the occurrence and intensity of these mechanisms.

Montgomery (Montgomery, 2013) stated that a successful design of experiments requires selection of a response variable(s) that provides useful information about the process under study. An important step in the design of experiments is identification of factors that may influence

* Corresponding author.
E-mail address: groll@purdue.edu (E.A. Groll).

https://doi.org/10.1016/j.ijrefrig.2023.03.016
Received 10 October 2022; Received in revised form 6 March 2023; Accepted 9 March 2023
Available online 15 March 2023

Nomenclature

air velocity	duct air velocity, m/s
HX	heat exchanger
D	deposition fraction, –
m	mass, kg

Greek letters

Δp	pressure drop, Pa

Subscripts

clean	clean condition
cumulative	cumulative
dep	deposited on heat exchanger
HX	heat exchanger
inc	incident on front face of heat exchanger
coil	coil or heat exchanger
d	dust
fouled	fouled condition at the end of a test run
i	counter for number of fouling periods

the performance of the process or system under study. These factors are classified into design factors, factors to be held constant, and factors that are allowed to vary. The sensitivity of the phenomenon to changes in operating conditions is the focus of the study. When an experiment is sensitive to changes in certain parameters, but their correlation is not of interest to the current study, their values are to be maintained constant during the experiment.

A high degree of control over air-side particulate fouling experiments is difficult to maintain, because many factors affect the phenomenon with potential correlation among factors. This complicates the classification of factors into the groups defined above. Different dimension scales exist in the experiment, *e.g.*, the foulant particle sizes may be micrometer-scale, whereas the heat exchanger dimensions may be on the scale of meters. This introduces complexity into the measurement as well. A possible solution is to separately study the phenomenon of particulate deposition on small sections of heat exchanger surfaces—such as that reported by Zhan *et al.* (F. Zhan et al., 2016) —and then to separately foul entire heat exchangers experimentally and measure the effect of fouling on the performance of the entire heat exchanger, as reported in this manuscript.

Using the proposed experimental protocol, a set of parametric experiments is designed to assess the extent of particulate fouling of a heat exchanger under operating conditions representative of those in the field, and the method of data reduction is explained. This proposed protocol is then implemented to obtain experimental results. The trends observed in the fouling behavior of the heat exchanger when certain operating parameters are varied are reported and analyzed.

2. Experiments

Experiments conducted as part of this research are a continuation of previous efforts that include Yang et al. (Yang et al., 2007), Bell and Groll (Bell and Groll, 2011), and Bell et al. (Bell et al., 2011). Experience gained from these earlier efforts in part informs the research conducted here.

2.1. Experimental setup

Fig. 1 shows the wind tunnel and the test stand used to generate the data reported in this study. The schematic is not to scale. The wind tunnel has been used in prior studies (Yang et al., 2007; Bell and Groll, 2011; Bell et al., 2011), with minor changes made for this study.

Additional information about the experimental setup is given in the supplementary material provided with this manuscript: S1.1 describes the wind tunnel and air-side components, S1.2 describes the water loop, and S1.3 explains the apparatus used to introduce the fouling agent into the air stream. Measurement instrumentation employed in this study is detailed in Section S1.4. Finally, Section S1.5 characterizes the fouling agent used in this study in accordance with Section 3.2 of Part 1 (Inamdar et al., 2023).

2.2. Choice of design parameters

The choice of which parameters to vary, and which to hold constant, is informed by data in the experimental literature as well as the theory of particulate deposition on heat transfer surfaces. Bott (Bott, 1988) presents an overview of the different mechanisms by which particulates deposit on heat transfer surfaces. Inertial impaction, an important

Table 1
Experimental parameters maintained constant for all experiments.

Experimental variable	Value	Unit
Air temperature at inlet to heat exchanger	2 4	°C
Water temperature at inlet to heat exchanger	6 0	°C
Mass flow rate of water	30	g/s
Total number of fouling periods	6	—
Duration of steady-state period	20	min

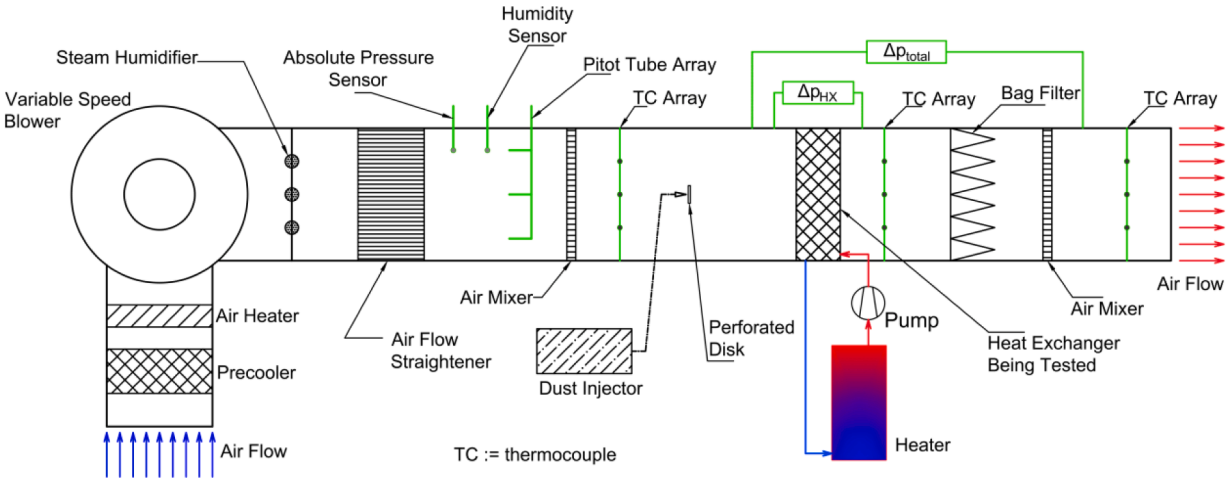

Fig. 1. Schematic diagram of the wind tunnel test setup used in this study to conduct fouling experiments.

Table 2
Test matrix for which measurements are reported in this work.

Test index		Relative humidity	Air velocity	Rate of dust injection	Duration of dust injection	Dust injected per fouling period	Total volume of airflow over the heat exchanger per fouling period	Dust concentration in air during fouling period
		%	m/s	g/h	min	g	m^3	mg/m^3
1	A	50	1.5	120	30	60	1003.4	59.8
	B			60	60		2006.7	29.9
	C†			15	240		8026.8	7.5
	D			7.5	480		16,053.6	3.7
2	A	60	1.0	100	60	100	1337.8	74.8
	B	70						
	C†	75						
	D	80						
	E†	90						
3	A	50	1.0	60	60	60	1337.8	44.8
	B		1.5	90	40			
	C		2.0	120	30			
	D†		2.5	150	24			

Table 3
Characteristics of the finned microchannel heat exchanger.

Dimension	Value	Unit
Finned width	609.6	mm
Finned height (total)	555.6	mm
Condenser section	400	mm
Subcooler section	155.6	mm
Finned depth	19	mm
Flat tube height		
Condenser section	1.09	mm
Subcooler section	3.0	mm
Fin density	3.74	cm^{-1}
Fin thickness	0.051	mm
Fin height	5.309	mm

mechanism in heat exchanger fouling, is a strong function of the velocity of airflow. Zhang et al. (Zhang et al., 1990) report that greater air velocities and greater bulk concentration of suspended particulates in the air stream both enhanced fouling on a finned-tube heat exchanger. Müller-Steinhagen et al. (Müller-Steinhagen et al., 1988) evaluated the effect of operating conditions including air velocity, particle size, and particulate concentration on fouling using a fouling probe. Admittedly, fouling probes are much different in geometry than heat exchangers, and therefore extrapolating from their data to heat exchangers is difficult. The overall fouling behavior was reported to be similar regardless of changes in operating conditions, and fouling resistance asymptotically reached a constant value. However, the magnitude and time required to reach this value was different for different cases. Bott and Bemrose (Bott and Bemrose, 1983) also varied air velocity and rate of dust injection in their experiments, but made no comparative observations.

Based on their experiments, Haghighi-Khoshkhoo and McCluskey (Haghighi-Khoshkhoo and McCluskey, 2007) observed the rate of introduction of dust into their wind tunnel to have no effect on the fouling process apart from duration to saturation, where saturation is the state at which no further change is observed in the total foulant deposition or the measured fouling resistance of the heat exchanger. An increase in concentration of suspended particulate in air flowing through the finned tube heat exchanger led to an accelerated accumulation of foulant deposition, as observed in Zhan et al. (F. Zhan et al., 2016). However, the total particle deposition weight per unit frontal area of heat exchanger reached approximately similar values asymptotically. Thus, the time required to reach a saturated state changed, but the saturation states did not show a large difference. A change in air velocity, on the other hand, led to different values of particle deposition weight per unit area of heat exchanger. A non-monotonic trend was reported, first promoting and then inhibiting particle deposition as air velocity increased.

Walmsley et al. (Walmsley et al., al.) held the humidity ratio constant at 60 g/kg in their experiments, but changed the air temperature at the inlet to the heat exchanger (maintaining a constant value per test run). The relative humidity correspondingly changed from 27% to 75% between test runs. From published photographs of their heat exchanger in the fouled condition, it is apparent that the severity of fouling deposition increases with an increase in relative humidity, and the sensitivity of this severity to a change in relative humidity is greater at larger values of relative humidity. They report that the adhesive nature of milk powder affected the severity of deposition and pressure drop increase.

The effect of changes in heat exchanger geometry such as the number of tube rows and fin pitch was compared in Pak et al. (Pak et al., 2005) and Yang et al. (Yang et al., 2007), while the differences between fouling of plate-finned-tube heat exchangers and finned-microchannel heat exchangers were investigated in Bell and Groll (Bell and Groll, 2011). Variation due to the choice of fouling agent is also reported in the literature; relevant studies are summarized in Part 1 (Inamdar et al., 2023). In the current study, a single heat exchanger geometry and fouling agent are used.

Based on these reported observations, the sensitivity of fouling to the concentration of suspended dust and air velocity is investigated in this study. Relative humidity at the inlet to the heat exchanger is chosen as the third parameter to be varied. Since the inlet air temperature is maintained constant, a change in relative humidity implies a proportional change in the humidity ratio, as long as ambient pressure does not vary significantly. Changes in air humidity could affect the characteristics of the layers of dust deposited on the heat exchanger such as porosity and the adhesive forces between the dust and the heat exchanger surface, thereby affecting deposition.

2.3. Experimental procedure

Some components used in the experimental setup are similar to those used in tests to characterize the efficacy of air-cleaning devices such as fibrous-media air filters—ANSI/ASHRAE Standard 52.2 (ANSI). However, the mechanisms by which these fibrous-media air filters arrest particulates in particulate-laden airflows are not the same as those by which particulates foul heat exchangers. Further, the adhesive forces between particulates and the fibrous media likely differ from those between particulates and metallic heat exchanger surfaces. Therefore, the experimental procedure described in Section 3.3 of Part 1 (Inamdar et al., 2023) is implemented instead of simply replicating the test procedure in ANSI/ASHRAE Standard 52.2. Briefly, the test procedure comprises a fouling period followed by a steady-state period, repeated in sequence. A pre-determined quantity of fouling agent is injected into the wind tunnel during the fouling period, and the heat exchanger is fouled. During the steady-state period, the performance of the heat exchanger in

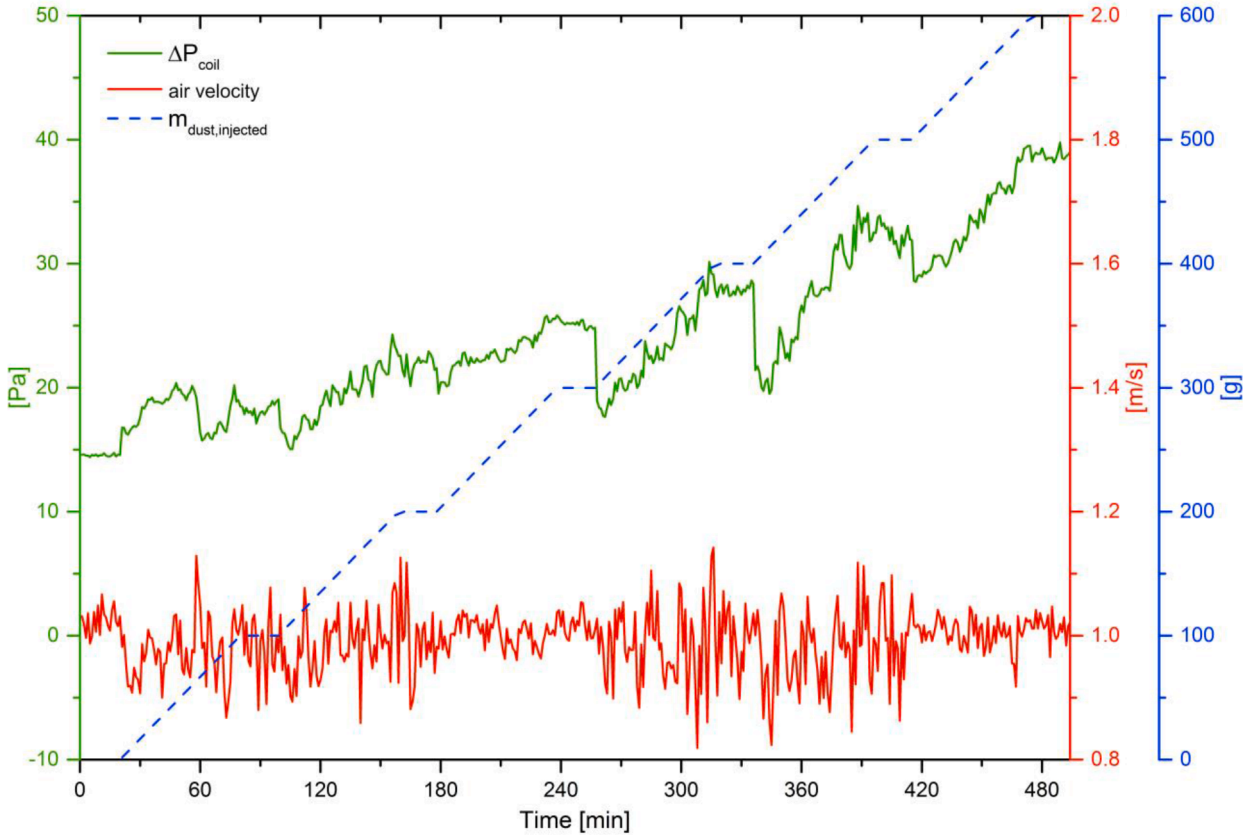

Fig. 2. Transient graph of total mass of dust injected into the air stream, air velocity, and associated pressure drop across heat exchanger (flow resistance) during all fouling and subsequent steady-state periods for Test Run 2B

the fouled condition is measured without further dust injection. The measurement during the steady-state period is assumed to correlate with the extent of fouling undergone by the heat exchanger in the preceding fouling period. At the end of the test, *i.e.* after the pre-determined number of fouling and subsequent steady-state periods are conducted, cleaning procedure(s) as described in Section 4 of Part 1 (Inamdar et al., 2023) are implemented to investigate their efficacy.

2.4. Test matrix

Three parameters are varied to evaluate their impact on heat exchanger fouling–air humidity, air velocity, and suspended particulate concentration. The test matrix is designed to vary one parameter while maintaining the other two constant. The total dust injected per fouling period is also maintained constant while varying each parameter, to eliminate any confounding effects of the differing amounts of prior foulant depositions on future heat exchanger fouling, which have been shown to accelerate heat exchanger fouling in previous research by Zhang et al. (Zhang et al., 1990), Mason et al. (Mason et al., 2006), and Moore (Moore, 2009). Therefore, the dust injected into the wind tunnel per fouling period is maintained constant within a test group. Table 1 lists experimental parameters that were maintained constant for all test cases in all test groups. Table 2 represents the fouling test matrix and the three main groups into which the experiments were divided, each varying one main parameter. Test runs marked with the symbol † were conducted twice to ascertain repeatability of the measurements and of the test procedure.

2.5. Heat exchanger cleaning procedure

At the end of a fouling test run, *in situ* cleaning procedures as described in Section 4 of Part 1 (Inamdar et al., 2023) are evaluated. Once the *in situ* cleaning sequence is complete, the modular heat exchanger section is unmounted from the wind tunnel, and thoroughly cleaned using hot water and a commercial coil cleaning agent intended for use on finned microchannel heat exchangers fabricated using aluminum (Nu-Calgon 2013).

2.6. Heat exchanger under investigation

The heat exchanger being tested as part of this research is an automotive condenser and has a finned microchannel design. On the refrigerant side, the heat exchanger is divided in two sections—the condenser (top) and the subcooler (bottom). The tube-side fluid enters the condenser section through a header and flows through the heat exchanger in a single pass. It then collects in a header on the other side of the heat exchanger and flows through the subcooler section in a single pass as well, and returns to the inlet side. The inlet and outlet headers are physically distinct. Characteristics of the heat exchanger are listed in Table 3.

3. Data analysis for fouling metrics

The deposition fraction as defined in Section 3.4 of Part 1 (Inamdar et al., 2023) is used to quantify the extent of air-side particulate fouling undergone by the heat exchanger.

When comparing test runs within a parametric group as defined in Table 2, the cumulative deposition fraction is used to quantify the total extent of fouling at the end of a complete test run. It is calculated according to:

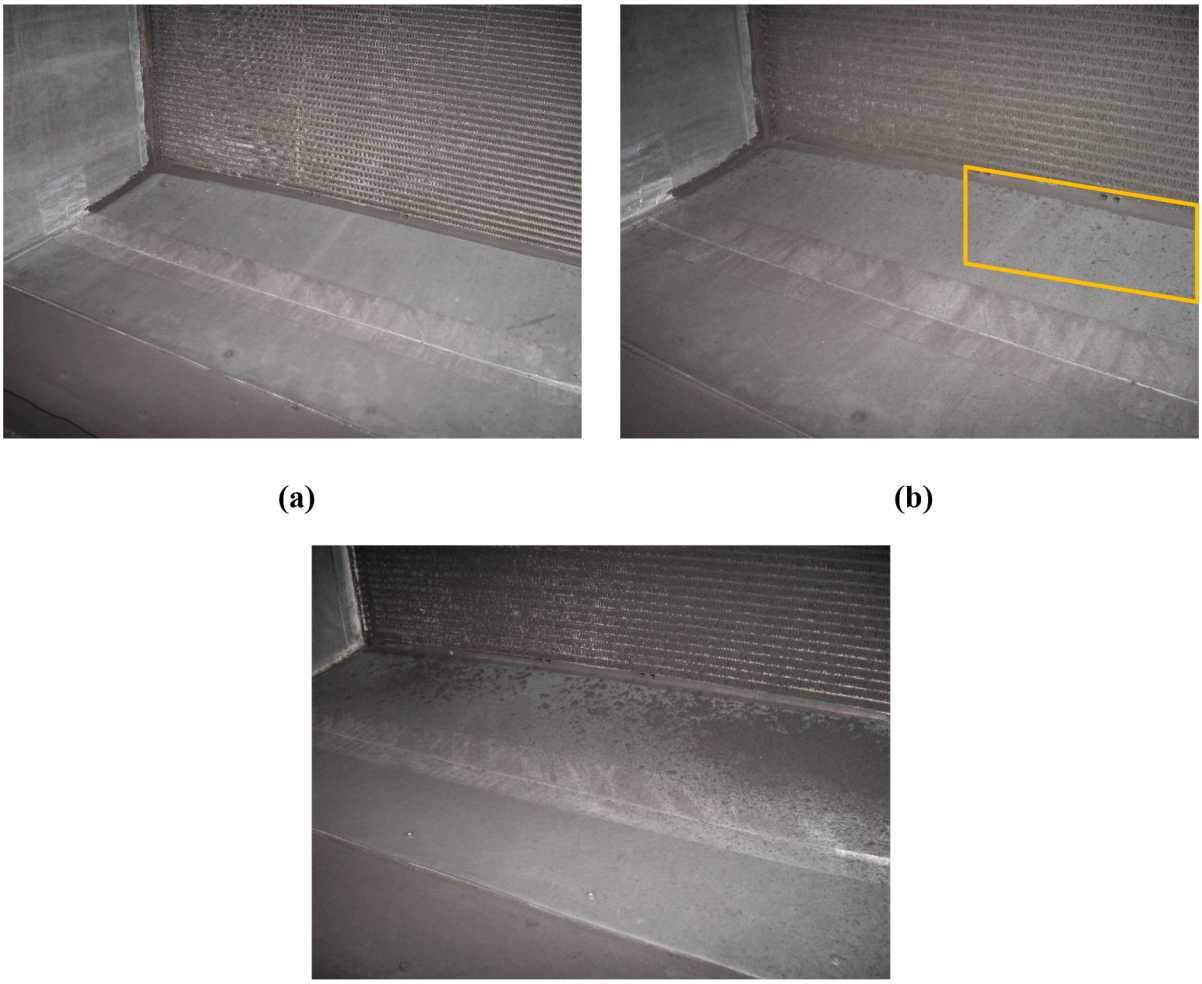

Fig. 3. Duct floor upstream of heat exchanger: (**a**) after first fouling period in Test Run 2B; (**b**) after sixth fouling period in Test Run 2B; and (**c**) after sixth fouling period in Test Run 2C.

$$D_{cumulative} = \frac{\sum_{i=1}^{6} \left(m_{d,dep}\right)_i}{\sum_{i=1}^{6} \left(m_{d,inc}\right)_i} \tag{1}$$

The impact of fouling is characterized in terms of the hydraulic resistance (specifically, the air-side pressure drop across the heat exchanger) and thermal resistance (specifically, the heat exchanger effectiveness). When comparing test runs within a parametric group in Table 2, the pressure drop and heat exchanger effectiveness values that correspond to a *fouled heat exchanger* are measured during the last steady-state period. Measurements denoted as corresponding to a *clean heat exchanger* are made during the zeroth steady-state period before any foulant is introduced. A comparison between these states is an indicator of the total degradation in the thermal and hydraulic performance of the heat exchanger due to fouling.

The data reduction procedure implemented to calculate heat exchanger effectiveness is reported in Sections S2.1 and S2.2 of the supplementary material; uncertainty analysis is explained in Section S2.3.

4. Test results

Experimental measurements reported in this section are for tests conducted per the test matrix described in Section 2.4. Detailed observations from Test Run 2B—including transient measurements—are reported in Section 4.1. Then, measurements from parametric test runs within groups defined in the test matrix in Table 2, Group 1 (change in rate of dust injection), Group 2 (change in relative humidity), and Group 3 (change in air velocity), are compared in Sections 4.3 to 4.5. Repeatability of the test protocol is discussed in Section 4.6.

All measured data reported in the section below control the blower motor speed to maintain a fix air velocity at the heat exchanger inlet. Section S3.1 of the supplementary material investigates fouling at a fixed blower speed (with a naturally reducing air velocity due to the increase in flow resistance due to fouling). Part 1 (Inamdar et al., 2023) proposed *in situ* cleaning methods that are experimentally assessed and reported in Section S3.2.

4.1. Detailed measurements for test run 2B

A plot of the measured air velocity, pressure drop across the heat exchanger, and mass of injected fouling agent with time is presented in Fig. 2. The abscissa is the running time of the test; the values plotted on the graph have been averaged over 1-min long intervals, as described in Section S2.1 of the supplementary material.

The plot shown in Fig. 2 has been stitched in time. The dust injector tray has a total travel time of 20 min before it must be reloaded. Thus,

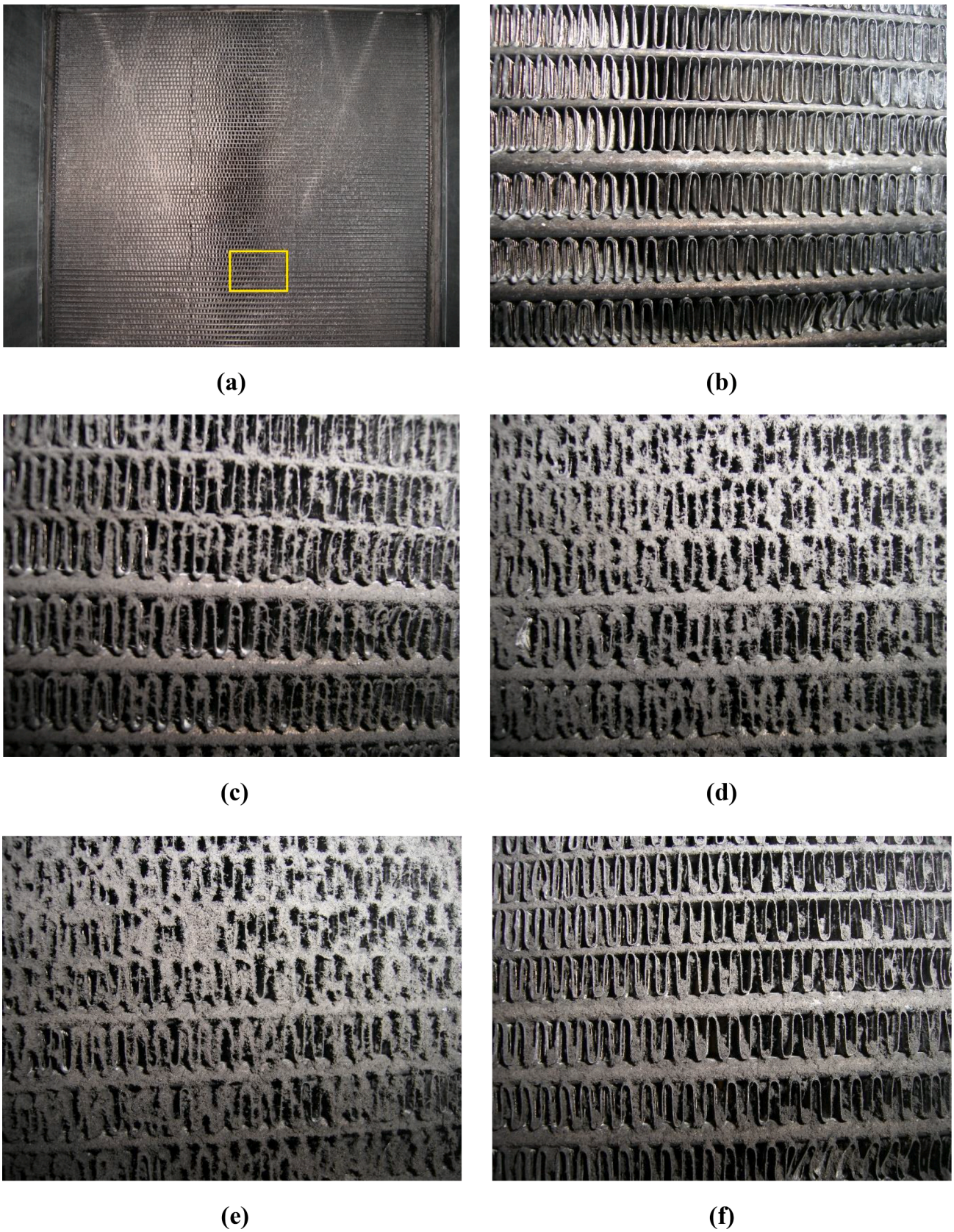

Fig. 4. Photographs of the front face of the heat exchanger from Test Run 2B: (**a**) location on the front face of which close-up photographs are provided; (**b**) clean heat exchanger; (**c**) after second fouling period; (**d**) after fourth fouling period; (**e**) after sixth fouling period; and (**f**) after *in situ* cleaning by reversal of airflow direction.

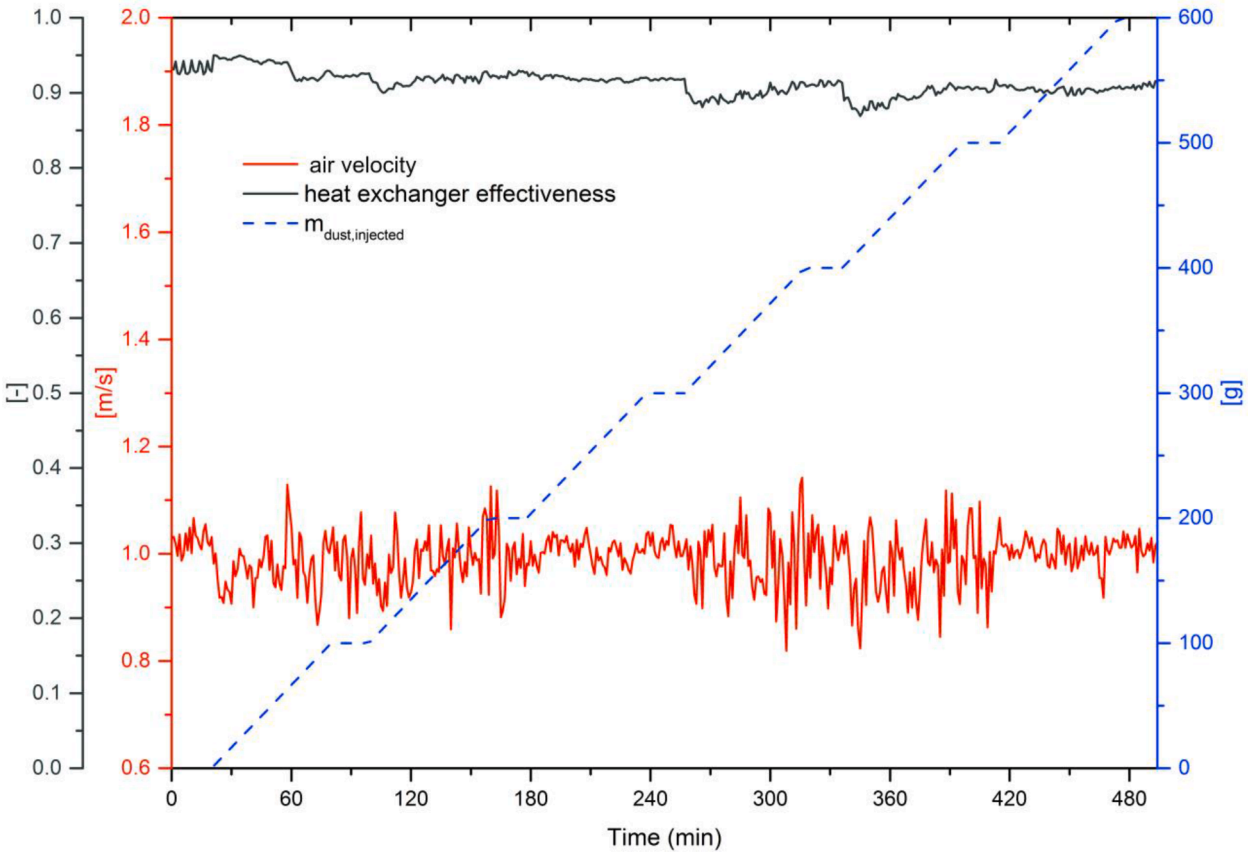

Fig. 5. Transient graph of total mass of dust injected into the air stream, air velocity, and associated heat exchanger effectiveness (thermal resistance) during all fouling and subsequent steady-state periods for Test Run 2B

Table 4
Efficacy of cleaning method during Test Run 2B

Cleaning method	Air velocity	Duration of cleaning procedure	Dust mass present on heat exchanger	Dust mass knocked off heat exchanger	Fraction of displaced dust
	m/s	min	g	g	%
Reversal of airflow direction	1.0	2	156.8	33.6	21.4

when fouling periods last longer than 20 min, the process of dust injection must be conducted in batches. When all the test dust from a batch has been injected into the air stream, a second batch of test dust is weighed and uniformly loaded on the tray. The airflow in the wind tunnel and the flow of hot water through the heat exchanger are maintained constant through this intermission. This intermission is kept as short as possible—below 5 min. This intermission is recorded during testing, and the raw data measured during such intermissions removed. The plot shown in Fig. 2 presents the data without intermissions.

Fouling periods can be identified as those regions where the slope of the plot corresponding to the mass of test dust injected into the air stream is positive. Steady-state periods are identified as those regions where the slope of this plot is zero. The first part of the plot from 0 min to 20 min is the steady-state measurement of the performance of the heat exchanger in clean condition. After 20 min, flows of air and water through the heat exchanger are stopped, and panels from the wind tunnel wall removed to weigh the bag filter and vacuum the duct floor upstream and downstream of the heat exchanger. Then, from time 20 min to 80 min is the first fouling period during which the mass of test dust injected into the wind tunnel increases from 0 g to 100 g. Air velocity and pressure drop fluctuate during the fouling period. The period from 80 min to 100 min is the first steady-state measurement of the performance of the heat exchanger in a fouled condition, as indicated by the plot for mass of dust injected into the air stream remaining constant at 100 g. At 100 min, flows of air and water through the heat exchanger are once again stopped to weigh the bag filter and vacuum the duct floor. As described in Table 2, the heat exchanger is fouled for 6 fouling periods, which from Table 3 last 60 min each. A steady-state period of 20 min follows each fouling period. Therefore, the entire test run lasts 500 min with a total 600 g of test dust injected into the air stream.

As airflow through the heat exchanger is stopped at the end of a steady-state measurement and restarted to begin the next fouling period, a marked drop is measured in pressure drop across the heat exchanger. It is likely that some test dust is held up against the front face of the heat exchanger by airflow in the wind tunnel. Once this airflow stops, these particles fall off the face of the heat exchanger, reducing the pressure drop they cause. Fig. 3 shows photographs of the duct floor immediately upstream of the front face of the heat exchanger. Such photographs are taken every time that airflow through the heat exchanger is stopped after a steady-state period. The photographs 2(a) and 2(b) are from Test Run 2B No dust is observed to be deposited on the duct floor upstream of the heat exchanger after the first fouling period, while a small quantity

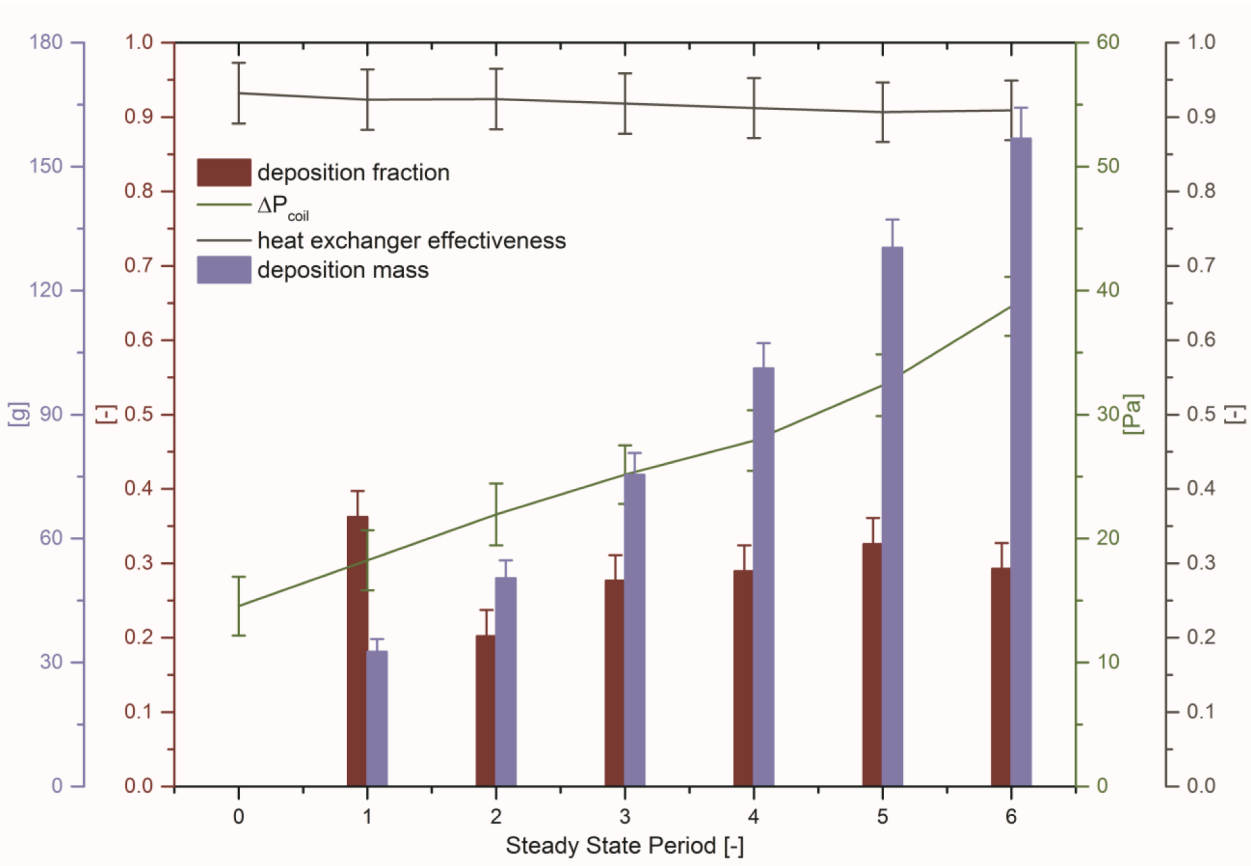

Fig. 6. Period-wise deposition fraction on the heat exchanger after each fouling period and subsequent pressure drop across (flow resistance) and heat exchanger effectiveness (thermal resistance) for the heat exchanger during each subsequent steady-state period for Test Run 2B

of test dust is seen after the sixth fouling period. A photograph from Test Run 2C is shown in 2(c) as a data point for an extreme case; most fouling tests show deposited test dust falling off the front face of the heat exchanger in a smaller quantity than in this case.

As expected from published data in the literature, the pressure drop measured across the heat exchanger increases monotonically as the total mass of dust injected into the air stream from the beginning of the test run increases. As dust deposits on the heat exchanger surface, flow area is blocked, and resistance to airflow increases. Since air velocity in the duct is maintained constant during this experiment, the pressure drop increases. Fig. 4 presents photographs taken of the front face of the heat exchanger at various times during the test run. Figure 4(a) shows the location on the front face of the heat exchanger that the other close-up photographs depict. Figure 4(b) shows the heat exchanger in clean condition, whereas Figures 4(c) through 4(e) show the progressive buildup of foulant deposition on the heat exchanger. Figure 4(f) shows the same location after *in situ* cleaning of the heat exchanger by reversal of airflow direction. It is seen that some of the deposition on the leading edges of fins and microchannel tubes is dislodged; however, foulant deposits are still seen inside the airflow channels.

Fig. 5 presents a transient plot of variables characterizing the thermal resistance of the heat exchanger, with the experimental data filtered as in Fig. 2. The mass of dust injected into the air stream in the wind tunnel increases during fouling periods and remains unchanged during steady-state periods. The heat exchanger effectiveness shows little change throughout the experiment.

The mass of test dust dislodged from the heat exchanger is measured following *in situ* cleaning. The efficacy of the cleaning procedure is characterized by the ratio of the mass of test dust removed from the heat exchanger to the mass of test dust present on the heat exchanger before cleaning. For Test Run 2B, statistics related to the cleaning methods are presented in Table 4.

After following the protocol for *in situ* cleaning as described in Part 1 (Inamdar et al., 2023), the heat exchanger section is removed from the wind tunnel and is cleaned as described in Section 2.5. From visual and mass-based assessment of the amount of foulant deposition still present on the heat exchanger, it is concluded that *in situ* cleaning is not sufficient to remove all foulant deposition, as can be achieved with a wet cleaning of the heat exchanger with coil cleaner. However, a non-negligible mass of dust can be simply removed *in situ* to regain some performance.

The performance of the heat exchanger during the steady-state periods is presented in Fig. 6. The total mass of foulant deposition present on the heat exchanger, as well as the pressure drop across the heat exchanger, increases after each fouling period. The pressure drop across the heat exchanger largely correlates with the increase in total mass of dust deposited on the heat exchanger. The change in the heat exchanger effectiveness after six fouling periods is within measurement uncertainty.

Air velocity at the front face of the heat exchanger is maintained constant during the test run by increasing the speed of the blower using a variable speed drive. It is hypothesized that the heat transfer performance of the heat exchanger does not change because the air velocity is maintained constant. Fouling may still potentially reduce the heat transfer surface area and increase thermal resistance due to the layer of foulant deposition. If a fixed speed blower motor were used, the airflow through the heat exchanger would decrease due to the increased pressure drop, consequently reducing the heat transfer rate. Measurements from a fixed speed blower test are reported in Section S3.1 of the supplementary material.

The deposition fraction is calculated for each fouling period independently and represents the rate of heat exchanger fouling during each

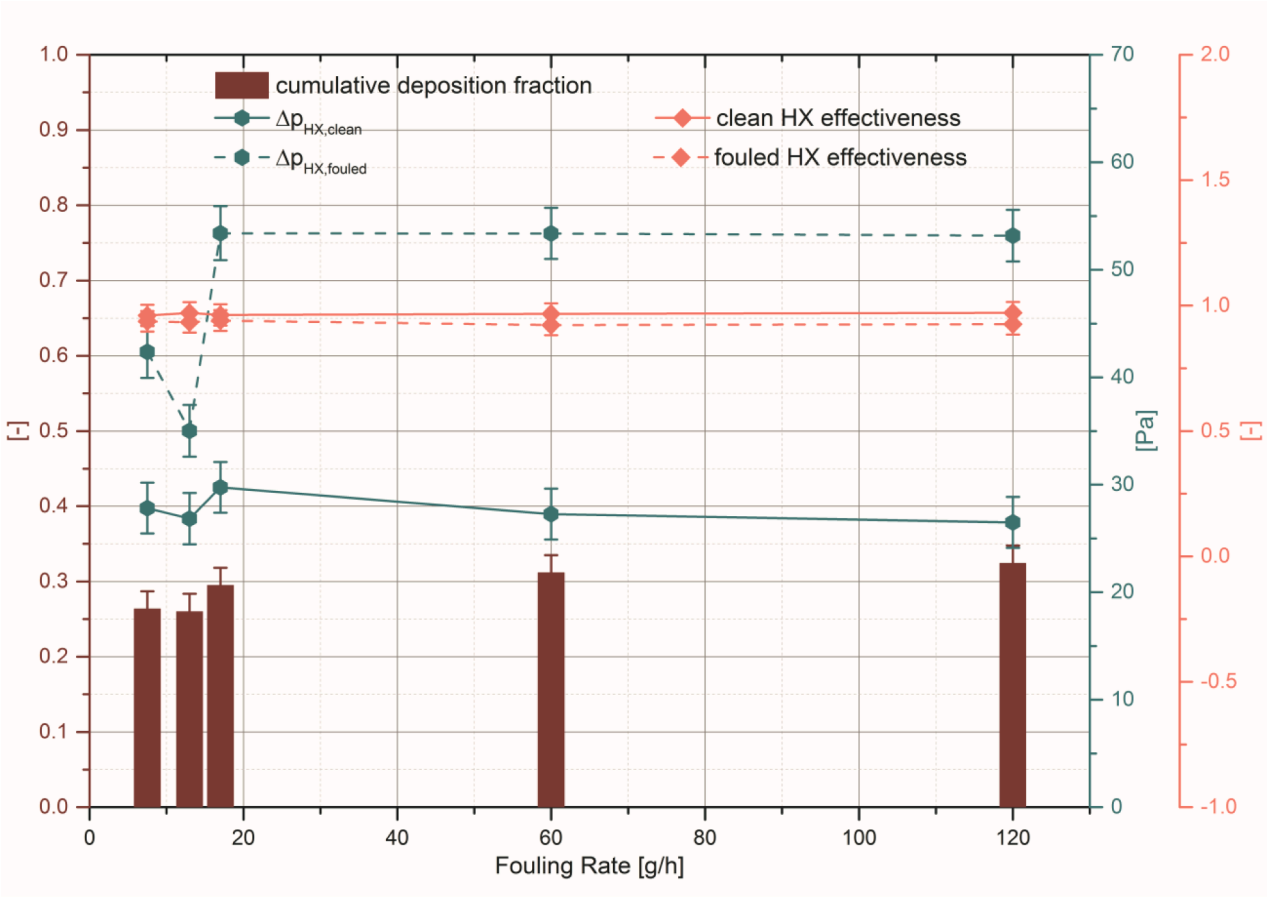

Fig. 7. Cumulative deposition fraction, pressure drop and heat exchanger effectiveness of clean heat exchanger and after the final (sixth) steady-state period of fouling for Group 1 (impact of variation in rate of dust injection) test runs. As summarized in Table 2, the fouling rates tested are 7.5, 15, 60, and 120 g/h; Test Run 1C at 15 g/h is repeated twice and the resulting data are shown as side-by-side bars.

(a) **(b)**

Fig. 8. Photographs of the front face of the heat exchanger at the end of: (**a**) Test Run 1A (foulant concentration 120 g/h); (**b**) Test Run 1D (foulant concentration 7.5 g/h).

fouling period. The deposition fraction for the first fouling period is observed to have the highest value; the value of deposition fraction for successive fouling periods is lower but does not show a monotonic trend. Nevertheless, it can be concluded that the fouling rate is initially high and subsequently decreases. This observation is repeated for all test runs.

The actual mass of dust deposited on the heat exchanger in the six successive fouling periods is 32.6, 17.8, 25.0, 25.8, 29.2, and 26.4 g. During every fouling period, approximately 10 g of dust out of the 60 g introduced into the wind tunnel by the dust injector is observed to fall out of suspension upstream of the heat exchanger. This is the sum of the dust that falls out of the air stream before ever reaching the front face of

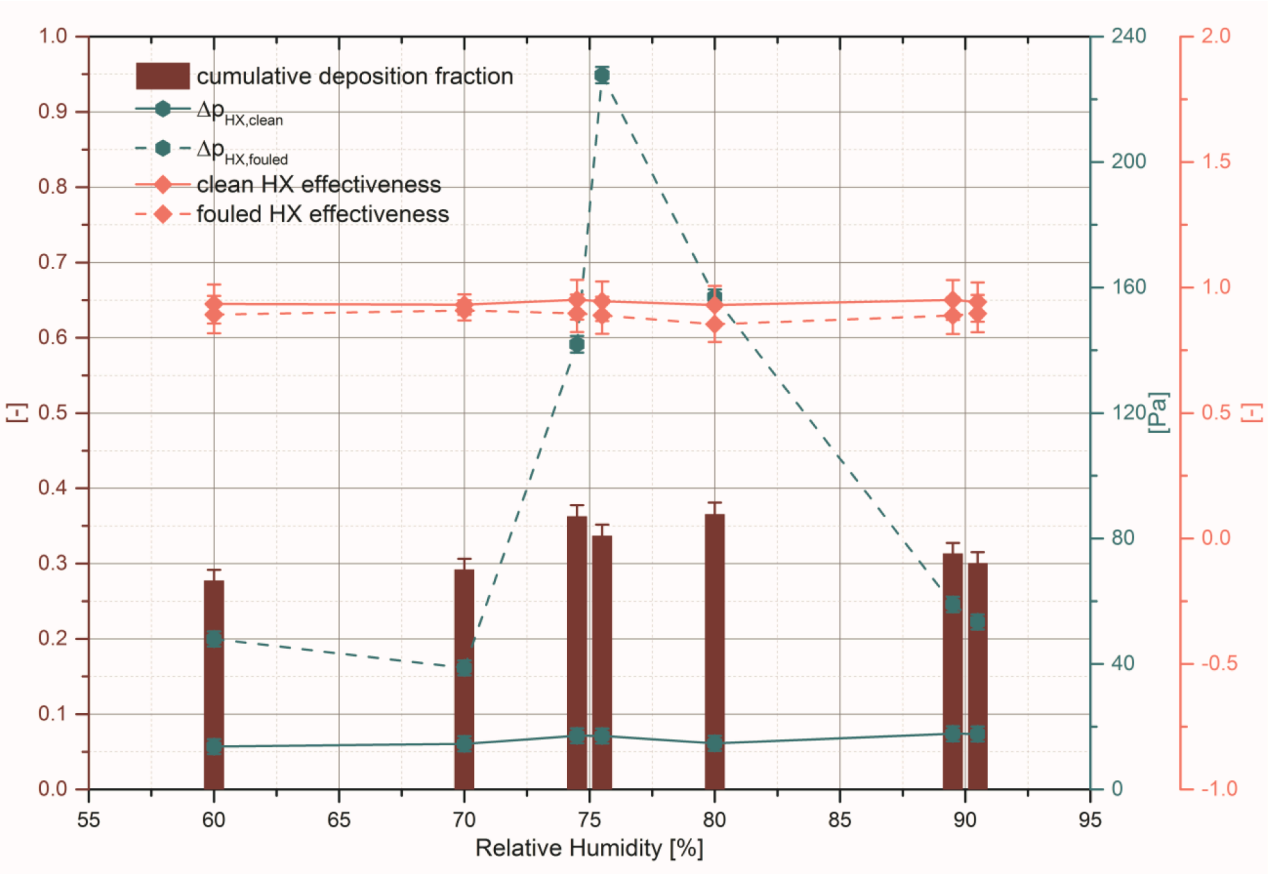

Fig. 9. Cumulative deposition fraction, pressure drop and heat exchanger effectiveness of clean heat exchanger and after the final (sixth) steady-state period of fouling for Group 2 (impact of variation in relative humidity) test runs. As summarized in Table 2, the relative humidity values tested are 60, 70, 75, 80, and 90%; Test Run 2C at 75% and Test Run 2E at 90% are repeated twice and the resulting data are shown as side-by-side bars.

the heat exchanger or is held against the front face of the heat exchanger but falls after airflow is stopped. The relatively constant value for successive fouling periods indicates a repeatable dust injection process. The mass of dust fallen out of suspension downstream of the heat exchanger is about 5 g per fouling period. Dust that passes through the heat exchanger without fouling could settle or dust already present on the heat exchanger could be knocked off. Both mechanisms may have contributed to this mass of dust on the duct floor downstream of the heat exchanger.

4.2. Parametric test runs

A comparison of measurements from test runs within each group defined in Table 2 is presented in Sections 4.3, 4.4, 4.5, and 4.6. As stated in Section 2.4, the total dust mass injected per test run is the same; therefore, the cumulative deposition fraction and total foulant deposition at the end of all test runs within a single group can be compared on an equal basis.

4.3. Effect on fouling of a change in dust concentration between test runs

A comparison of experimental measurements from Group 1 (Table 2) for different dust injection rates is presented in Fig. 7. For all test runs, the measured pressure drop across a fouled heat exchanger is greater than across a clean heat exchanger. As air velocity is maintained constant despite fouling, the measured heat exchanger effectiveness is negligibly different for a clean and fouled heat exchanger.

When assessing the impact of an increase in foulant concentration (concentration of dust in air), it is seen that the cumulative deposition fraction is higher for the three highest foulant concentrations. The change in cumulative deposition fraction is not observed to significantly affect heat exchanger effectiveness; pressure drop across the fouled heat exchanger correlates with the cumulative deposition fraction.

As a qualitative assessment of the deposition, Fig. 8 compares photographs of the front face of the heat exchanger after the last steady-state period at the end of the test run for cases with lowest (Test Run 1A; 120 g/h) and highest (Test Run 1D; 7.5 g/h) foulant concentrations. Deposition appears to occur to a larger extent in the test run with the higher foulant concentration.

4.4. Effect on fouling of a change in relative humidity between test runs

A comparison of experimental measurements from Group 2 (Table 2) of test runs is presented in Fig. 9. Again, pressure drop across a fouled heat exchanger is notably greater than that across a clean heat exchanger, but the heat transfer effectiveness is negligibly reduced after

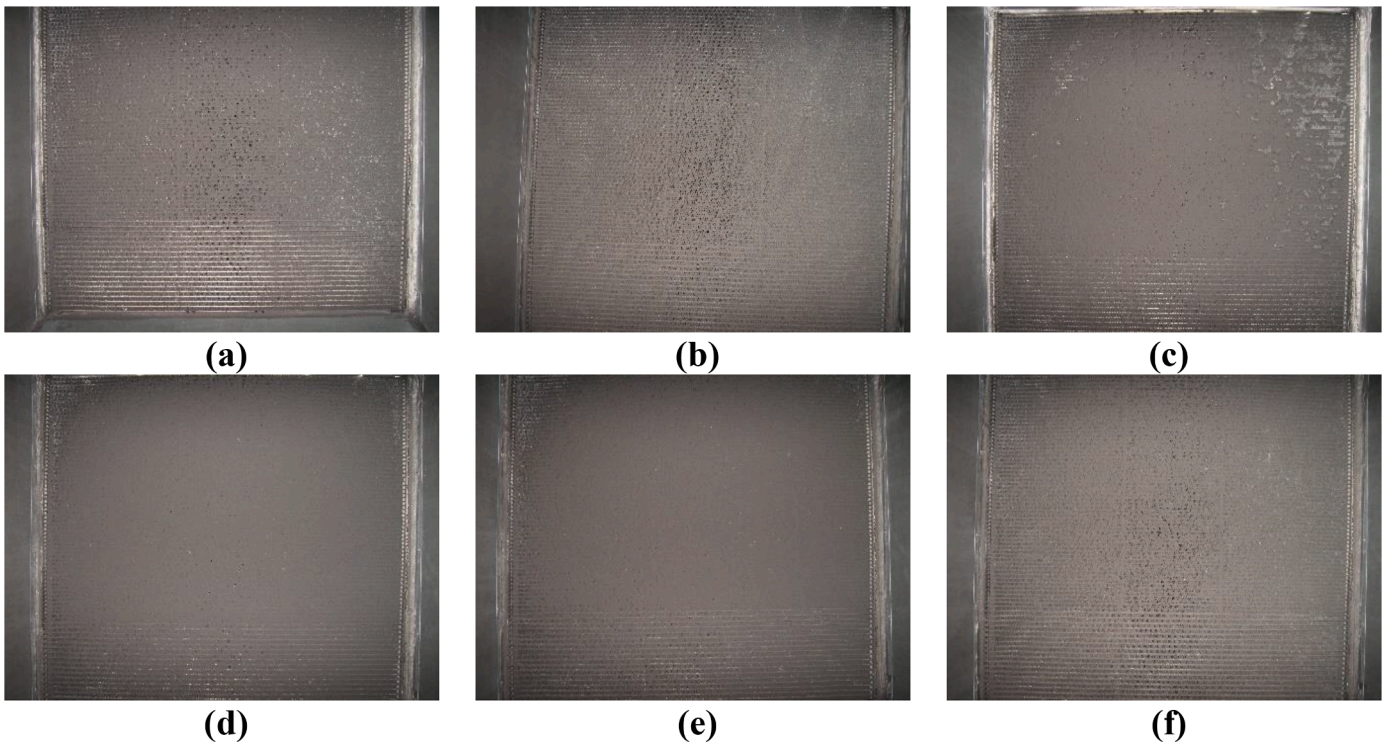

Fig. 10. Photographs of the front face of the heat exchanger at the end of: (**a**) Test Run 2A (60% relative humidity); (**b**) Test Run 2B (70% relative humidity); (**c**) Test Run 2C (75% relative humidity), with lower measure pressure drop; (**d**) repeated Test Run 2C (75% relative humidity), with higher measured pressure drop; (**e**) Test Run 2D (80% relative humidity); and (**f**) Test Run 2E (90% relative humidity), with higher measured pressure drop.

fouling. The pressure drop across the fouled heat exchanger roughly correlates with the cumulative deposition fraction.

It is observed that the cumulative deposition fraction tends to peak at an intermediate relative humidity value near 75% to 80%, with a lower deposition fraction at both lower and higher humidity of air at heat exchanger inlet.

A series of photographs are presented in Fig. 10, showing the front face of the heat exchanger after the last fouling period for test runs from Group 2. Foulant deposition is observed on a larger face area of the heat exchanger in photographs for Test Runs 2C (relative humidity 75%) and 2D (relative humidity 80%), compared to other test runs. While these photographs provide qualitative verification of measured cumulative deposition fractions, it is important to note that they only show dust deposited on the front face of the heat exchanger and not inside the airflow channels. Nevertheless, the difference between foulant deposition at the end of different test runs is evident in Fig. 10.

It is reiterated that all photographs in Fig. 10 are captured and quantitative measurement of foulant deposition is conducted after airflow is stopped, but pressure drop across the fouled heat exchanger and heat exchanger effectiveness are measured during steady-state periods directly following fouling periods without stopping airflow. A second set of photographs is presented in Fig. 11 to show the duct floor directly upstream of the heat exchanger after airflow is stopped at the end of a test run. The region of the wind tunnel floor in the photographs is as wide as the front face of the heat exchanger and extends about 0.1 m (4 inches) upstream from its front face. It is hypothesized that most of the dust on the floor in this region is held up against the frontal edges of fins and tubes and falls out of suspension once airflow stops.

4.5. *Effect on fouling of a change in air velocity between test runs*

A comparison of experimental measurements from Group 3 (Table 2) of test runs is presented in Fig. 12. The trend of pressure drop across a fouled heat exchanger being higher than across a clean heat exchanger is consistent in this group of measurements too; there is an insignificant difference in heat exchanger effectiveness for a fouled *versus* a clean heat exchanger.

As the face air velocity increases, the cumulative deposition fraction reduces. The pressure drop across the fouled heat exchanger correlates with the total mass of foulant deposition on the heat exchanger surface.

Photographs of the front face of the heat exchanger after the last steady-state period are presented for Test Run 3A (1.0 m/s) and both iterations of Test Run 3D (2.5 m/s) in Fig. 13. The decrease in severity of fouling for Test Run 3D *versus* Test Run 3A, as reported in Fig. 12 through a reduced cumulative deposition fraction, is mirrored in these photographs.

4.6. *Repeatability of experimental data*

Several test cases described in the above sections were repeated to assess the repeatability of measurements. From Group 1 (Table 2), Test Run 1C (15 g/h) is repeated (Fig. 7); from Group 2 (Table 2), Test Run 2C (75% relative humidity) and Test Run 2E (90% relative humidity) are repeated (Fig. 9); and from Group 3 (Table 2), Test Run 3D (2.5 m/s) is

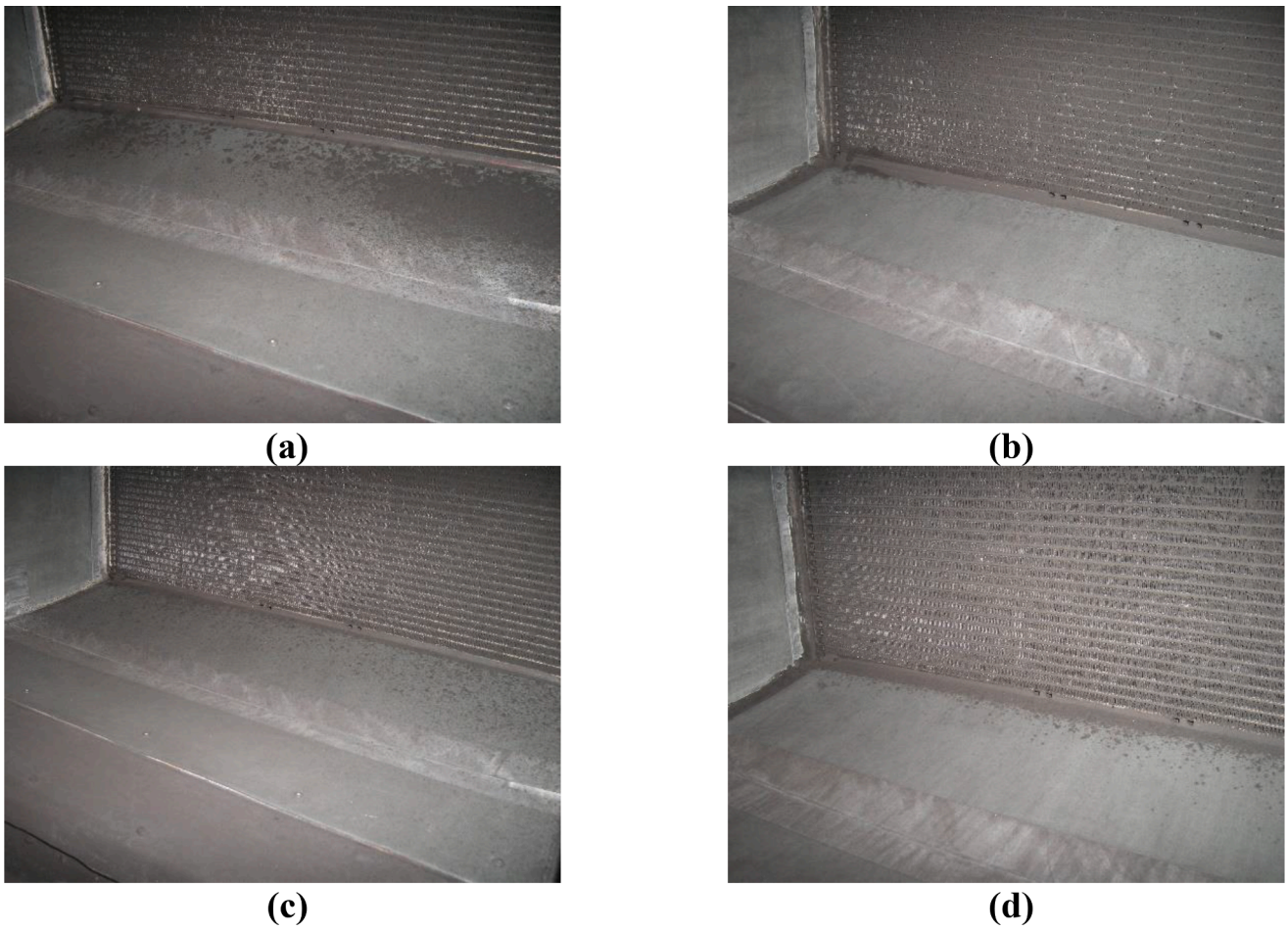

Fig. 11. Photographs of the duct floor immediately upstream of the heat exchanger at the end of: (**a**) Test Run 2C, with lower measure pressure drop; (**b**) repeated Test Run 2C, with higher measured pressure drop; (**c**) Test Run 2E, with higher measured pressure drop; and (**d**) Test Run 2E, with lower measured pressure drop.

repeated (Fig. 12). Across all of these comparisons, the pressure drop across the clean heat exchangers were very repeatable, but slight differences in the cumulative deposition fractions for repeated tests led to some differences in the measured pressure drop values across the fouled heat exchanger at the end of the respective test runs, outside the experimental uncertainty. These differences can be attributed to known batch-to-batch variation in the physical properties of the standardized fouling agent (test dust). Consistency of the fouling agent is discussed further in Section S4.1 of the supplementary material.

Two additional factors of note for those looking to perform such fouling experiments relate to the blower (discussed in Section S4.2) and filter (discussed in Section S4.3) selection. The blower should be selected to avoid operation at pressure heads that may lie in unstable regions of the fan curve in a blow-through airflow configuration, which leads to fluctuations in the air velocity as observed in the current experiments. Additionally, the bag filter should be selected to have a high arrestance efficiency over the entire particle size range of the fouling agent.

5. Conclusion

A finned microchannel heat exchanger is experimentally investigated to demonstrate implementation of an experimental test protocol to assess particulate fouling of heat exchangers proposed in Part 1 (Inamdar et al., 2023). A set of parametric experiments is designed based on this protocol. A method of data reduction is proposed to calculate fouling metrics. Measurements made during the parametric testing are reported and some inferences regarding particulate fouling are drawn.

The efficacy of the experimental protocol can be assessed based on the consistency of experimental data produced and the utility of these data in making predictions about the observed phenomena. The measurements reported here, utilizing the proposed protocol, show the effect of changes in operating conditions on particulate fouling. As identified from an exhaustive review of the literature, past data on particulate fouling of heat exchangers demonstrates apparent contradictions due to differences in testing protocol and the inherent complexity of the fouling process. Generating and reporting data following this proposed protocol may allow for reconciliation and consensus between researchers regarding the role of operating conditions on air-side particulate fouling of heat exchangers.

Declaration of Competing Interest

The authors declare that they have no known competing financial interests or personal relationships that could have appeared to influence the work reported in this paper.

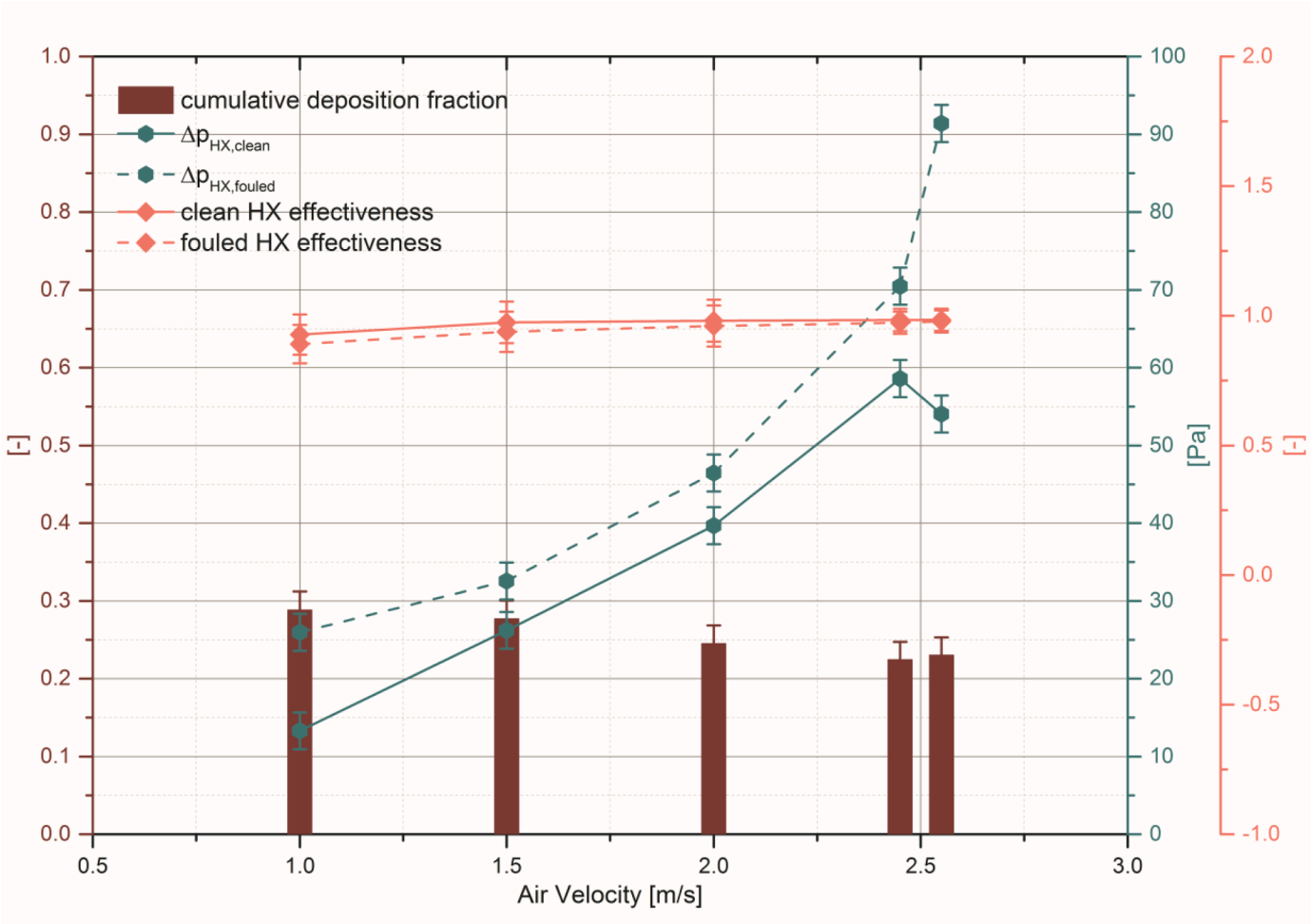

Fig. 12. Cumulative deposition fraction, pressure drop and heat exchanger effectiveness of clean heat exchanger and after the final (sixth) steady-state period of fouling for Group 3 (impact of variation in air velocity) test runs. As summarized in Table 2, the air velocities tested are 1.0, 1.5, 2.0, and 2.5 m/s; Test Run 3D at 2.5 m/s is repeated twice and the resulting data are shown as side-by-side bars.

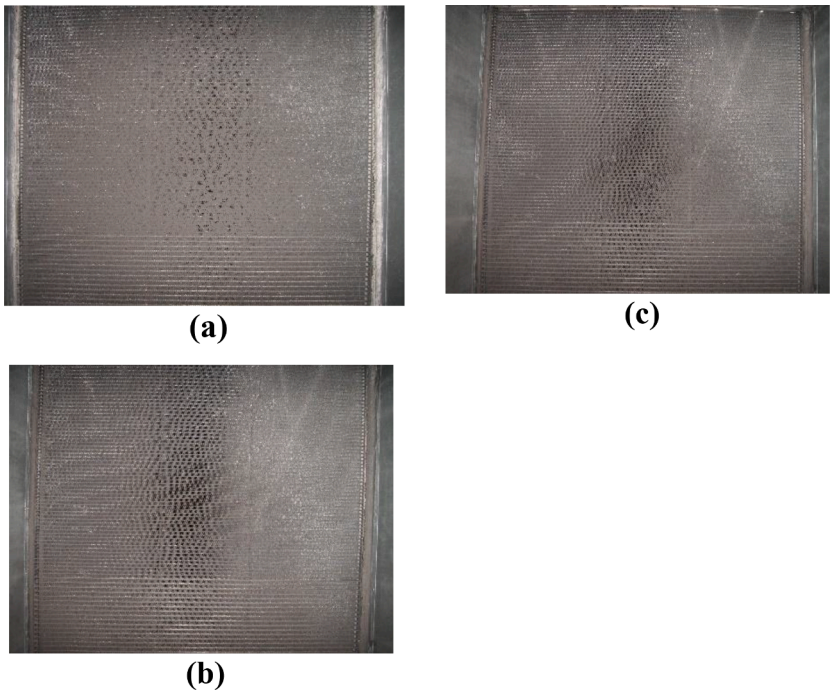

Fig. 13. Photographs of the front face of the heat exchanger at the end of: (**a**) Test Run 3A (1.0 m/s); (**b**) Test Run 3D (2.5 m/s), with lower measured pressure drop; and (**c**) repeated Test Run 3D (2.5 m/s), with larger measured pressure drop.

Acknowledgement

This study was partially funded by members of the Cooling Technologies Research Center, an NSF Industry/University Cooperative Research Center at Purdue University. The heat exchanger tested in this research was donated by Denso Corporation. The support provided by the staff of Ray W. Herrick Laboratories in the experimentation phase is gratefully acknowledged.

Supplementary materials

Supplementary material associated with this article can be found, in the online version, at doi:10.1016/j.ijrefrig.2023.03.016.

References

Bell, I.H., Groll, E.A., 2011. Air-side particulate fouling of microchannel heat exchangers: experimental comparison of air-side pressure drop and heat transfer with plate-fin heat exchanger. Appl. Therm. Eng. 31 (5), 742–749. https://doi.org/10.1016/j.applthermaleng.2010.10.019.

Bell, I.H., Groll, E.A., König, H., 2011. Experimental analysis of the effects of particulate fouling on heat exchanger heat transfer and air-side pressure drop for a hybrid dry cooler. Heat Transfer Eng. 32 (3/4), 264–271. https://doi.org/10.1080/01457632.2010.495618.

Bott, T.R., 1988. Gas side fouling. In: Melo, L.F., Bott, T.R., Bernardo, C.A. (Eds.), *Fouling Science and Technology* (191–203). Kluwer Academic Publishers, Dordrecht. https://doi.org/10.1007/978-94-009-2813-8.

Bott, T.R. (1995). *Fouling of heat exchangers*. doi:10.1016/b978-0-444-82186-7.x5000-3.

Bott, T.R., Bemrose, C.R., 1983. Particulate fouling on the gas-side of finned tube heat exchangers. J. Heat Transfer 105 (1), 178–183. https://doi.org/10.1115/1.3245538.

Haghighi-Khoshkhoo, R., McCluskey, F.M.J., 2007. Air-side fouling of compact heat exchangers for discrete particle size ranges. Heat Transfer Eng. 28 (1), 58–64. https://doi.org/10.1080/01457630600985675.

Inamdar, H.V., Groll, E.A., Weibel, J.A., Garimella, S.V., 2023. Air-side Fouling of Finned Heat Exchangers: Part 1, Review and Proposed Test Protocol. Int. J. Refrig. https://doi.org/10.1016/j.ijrefrig.2023.02.017.

Mason, D.J., Douch, N., Heikal, M.R., 2006. Air side fouling of compact heat exchangers. Int. J. Heat Exch. 7 (1), 1–14. ISSN:15245608.

Method of Testing General Ventilation Air-Cleaning Devices For Removal Efficiency By Particle Size. (ANSI/ASHRAE Standard 52.2–2012). Atlanta, GA: American Society of Heating, Refrigerating, and Air-Conditioning Engineers, Inc.

Montgomery, D.C. (2013). *Design and analysis of experiments* (8th ed.). Retrieved from http://www.wiley.com/WileyCDA/WileyTitle/productCd-EHEP002024.html. ISBN: 978-1-118-32426-4.

Moore, D.A., 2009. Characterization of fiber accumulation fouling in fine pitched heat sinks. In: Proceedings of the 25th Semiconductor Thermal Measurement and Management Symposium, San Jose, CA. IEEE, Piscataway, NJ, pp. 279–284. https://doi.org/10.1109/STHERM.2009.4810776.

Müller-Steinhagen, H., Reif, F., Epstein, M., Watkinson, A.,P., 1988. Influence of operating conditions on particulate fouling. Can. J. Chem. Eng. 66 (1), 42–50. https://doi.org/10.1002/cjce.5450660106.

Nu-Calgon. (2013, October 28). *Safety Data Sheet for Cal-Green*. Retrieved from Nu-Calgon Wholesaler, Inc.'s website: http://www.nucalgon.com/assets/SDS/English/4190_SDS_ENG.pdf. Retrieved on April 1, 2017.

Pak, B.C., Groll, E.A., Braun, J.E., 2005. Impact of fouling and cleaning on plate fin and spine fin heat exchanger performance. ASHRAE Trans. 111 (1), 496–505. ISSN:0001-2505.

Walmsley, T.G., Walmsley, M.R.W., Atkins, M.J., & Neale, J.R. Fouling and pressure drop analysis of milk powder deposition on the front of parallel fins. *Adv. Powder Technol.,* 24(4), 780–785. doi:10.1016/j.apt.2013.04.004.

Yang, L., Braun, J.E., Groll, E.A., 2007. The impact of fouling on the performance of filter–evaporator combinations. Int. J. Refrig. 30 (3), 489–498. https://doi.org/10.1016/j.ijrefrig.2006.08.006.

Zhan, F., Tang, J., Ding, G., Zhuang, D., 2016a. Experimental investigation on particle deposition characteristics of wavy fin-and-tube heat exchangers. Appl. Therm. Eng. 99, 1039–1047. https://doi.org/10.1016/j.applthermaleng.2016.01.136.

Zhang, G., Bott, T.R., Bemrose, C.R., 1990. Finned tube heat exchanger fouling by particles. In: Proceedings of *International Heat Transfer Conference 9, Jerusalem, Israel*. Begell House Publishers, Danbury, CT, pp. 115–120. Section: Heat ExchangersOCLC: 439777445.

Zhan, F., Tang, J., Ding, G., Zhuang, D., 2016b. Experimental investigation on particle deposition characteristics of wavy fin–and–tube heat exchangers. Appl. Therm. Eng. 99, 1039–1047. https://doi.org/10.1016/j.applthermaleng.2016.01.136.